Supporting Information (SI)

DFT Study on the Methanol Decomposition over $Pt/CeO_2(110)$ catalysts: effect of size and position of Pt

Hao Lu,[a,⊥] Yuan Zhong,[a,⊥] Yao Jie,[a] Pan Yin,[a] Xiao-Jie Zhao,[a] Yu-Liang Feng,[a] Tian-Yao Shen,[a] Jing-Yi Guo,[a] Wei Zhang,[a] Min Pu,[a] Hong Yan,*[a]

[a] *State Key Laboratory of Chemical Resource Engineering, College of Chemistry, Beijing University of Chemical Technology, Beijing 100029, China*

***** Corresponding Authors:

yanhong@mail.buct.edu.cn (Hong Yan).

⊥Hao Lu and Yuan Zhong contributed equally to this work.

Contents

1. The calculation of the surface energy.

Surface energy (SE) is defined as the amount of energy required to cleave an infinite crystal into two parts, i.e. the energy required to form a new surface. It is calculated as shown in Eq 1:

$$E_{surf} = \frac{1}{2A}(E_{slab} - E_{bulk}) \tag{1}$$

where E_{slab} is the total energy of the slab, E_{bulk} is the energy in the bulk. In general, it is known that the smaller the surface energy is, the easier is to form a surface, i.e., the surface with smaller surface energy is easier to be exposed.

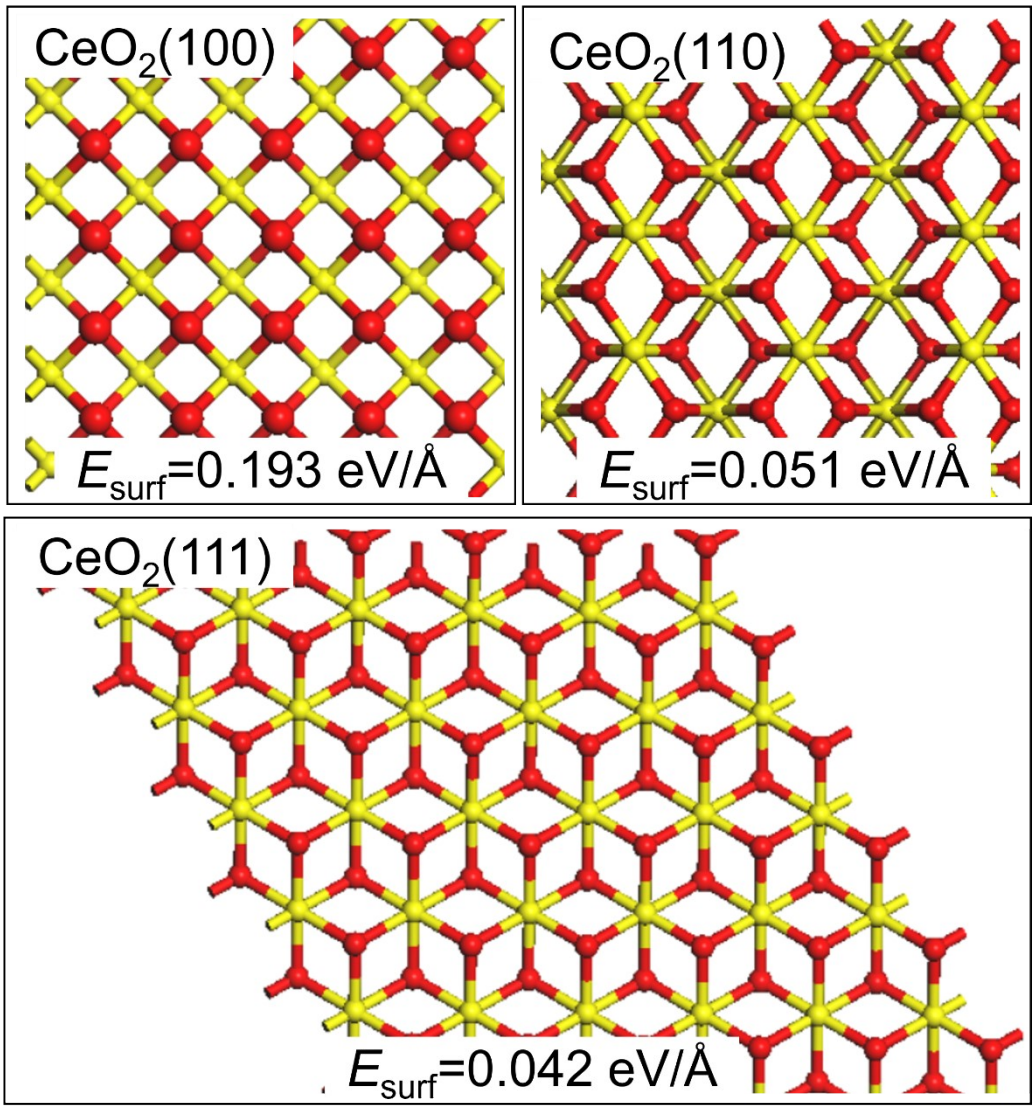

Figure S1. The top view of the optimized structures of $CeO_2(100)$, $CeO_2(110)$ and $CeO_2(111)$ surfaces. O: red; Ce: yellow.

2. Energy test for *k*-point.

Table S1. Binding energy (*BE*) of the Pt atom on $CeO_2(110)$ surface (in eV) when *k*-point are 3×3×1 and 5×5×1, respectively

k-point	E_{slab}/eV	E_{Pt}/eV	E_{total}/eV	*BE*/eV
3×3×1	–408.747	–0.570	–412.013	–2.696
5×5×1	–408.747	–0.570	–412.012	–2.695

As shown in Table S1, binding energies (*BE*) of the Pt atom with the support $CeO_2(110)$ are calculated. When the *k*-point is set to 3×3×1, the binding energy is –2.696 eV, and when the *k*-point is increased to 5×5×1, the binding energy has only a small change (0.001 eV). Therefore, in order to save computing resources, the *k*-point of 3×3×1 is used to complete all calculations.

3. Energy test for cut-off energy (ENCUT).

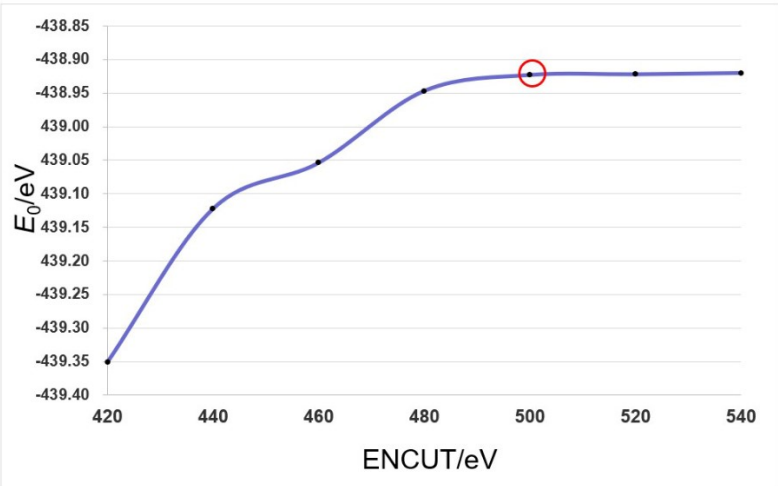

Figure S2. Take the energy E_0 of CH_3OH adsorbed on $CeO_2(110)$ surface as an

example for ENCUT test.

In order to make reasonable use of computing resources, we tested the cutoff energy (ENCUT) required for the calculation. If the ENCUT value is too small, the system will be difficult to converge, and if it is too large, it will take longer to waste computing resources. As shown in Figure S2, for the system we want to study, when the ENCUT value is 500 eV, it can not only ensure the convergence of the system, but also save computing resources.

4. Energy test for supercell size

Table S2. Adsorption energy of methanol molecules on $Pt/CeO_2(110)(2\times1)$ and $Pt/CeO_2(110)(2\times2)$ (Unit: eV)

CeO_2 supercell	Adsorption energy of methanol molecules(eV)		
	$Pt_1/CeO_2(110)$	$Pt_7/CeO_2(110)$	$Pt_1/Ce_{1-x}O_2(110)$
2×1	–1.173	–0.996	–0.737
2×2	–1.194	–0.987	–0.721

As shown in Table S2, a very small difference(about 0.02eV) in adsorption energy on supercell $CeO_2(110)(2\times1)$ and supercell $CeO_2(110)(2\times2)$. Therefore, in order to save computing resources, $CeO_2(110)(2\times1)$ is used to complete all calculations.

5. Screening of the Pt sites.

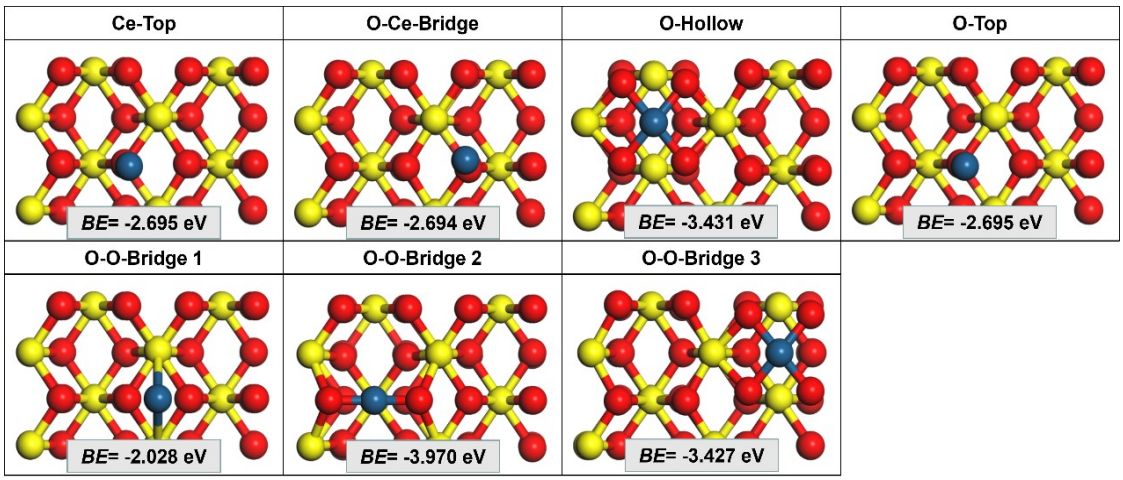

Figure S3. Pt single-atom binding site screening of $Pt_1/CeO_2(110)$. O: red; Ce: yellow; Pt: blue.

As shown in Figure S3, a total of 7 Pt single-atom binding sites were screened, and the figure shows the optimized model of the initial structure of each site, excluding O-O-bridge 1, which has the lowest binding energy, and OO-bridge 2, which has severe deformation. Both Ce-top and O-Ce-bridge tend to bind to the oxygen site, and O-O-bridge 3 tends to bind to the O-hol site. The final comparison between the O-top and O-hol sites, and the optimal adsorption energy of CH_3OH on the O-Hol and O-Top models are -0.250 eV and -1.173 eV, respectively. Therefore, the O-Top site is the best binding site.

6. Size screening of Pt_n clusters on $CeO_2(110)$.

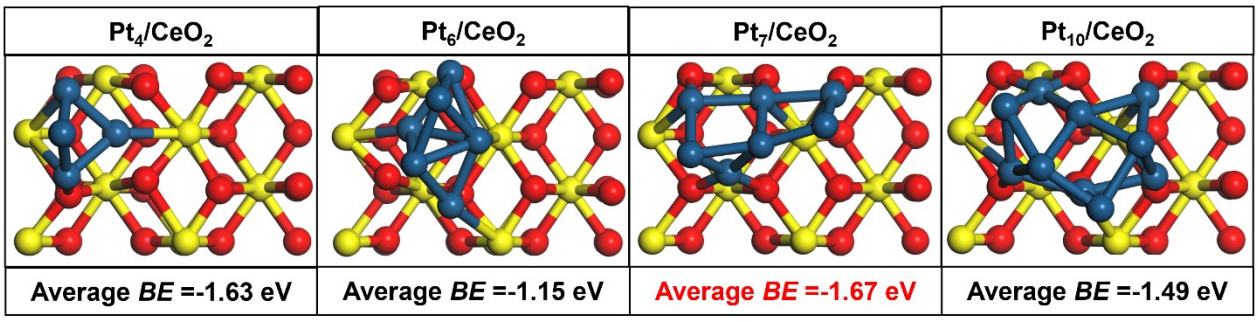

Figure S4. Comparison of average binding energies (*BE*) of Pt_4, Pt_6, Pt_7 and Pt_{10}

clusters loaded on CeO_2(110). O: red; Ce: yellow; Pt: blue.

Average *BE* indicates the average binding energies (*BE*) of the Pt atoms bonded to CeO_2(110) (Average $BE = \frac{BE}{N_{Pt}}$). As shown in Figure S4, the Pt_7 cluster has the largest Average *BE* (-1.67 eV), which indicates that the Pt_7 cluster is the most stable on the CeO_2(110), therefore the Pt_7/CeO_2(110) model is finally chosen.

7. Screening of methanol molecular adsorption sites.

As shown in Figure S5, five possible adsorption configurations are calculated (O-Top, Ce-Top, O-O-Bri, O-Ce-Bri, Pt-Top, and Pt-Pt-Bri sites). The interfacial adsorption sites of methanol on Pt_1/CeO_2(110) and Pt_7/CeO_2(110) are also screened, and the adsorption energy of methanol molecules at the interfacial sites is very small, and a methanol molecule runs to the surface site of the Pt atom after structural optimization (O-Top site on Pt_1/CeO_2(110)). This indicates that the interface of CeO_2 with the Pt atom/cluster has no significant effect on the elementary steps.

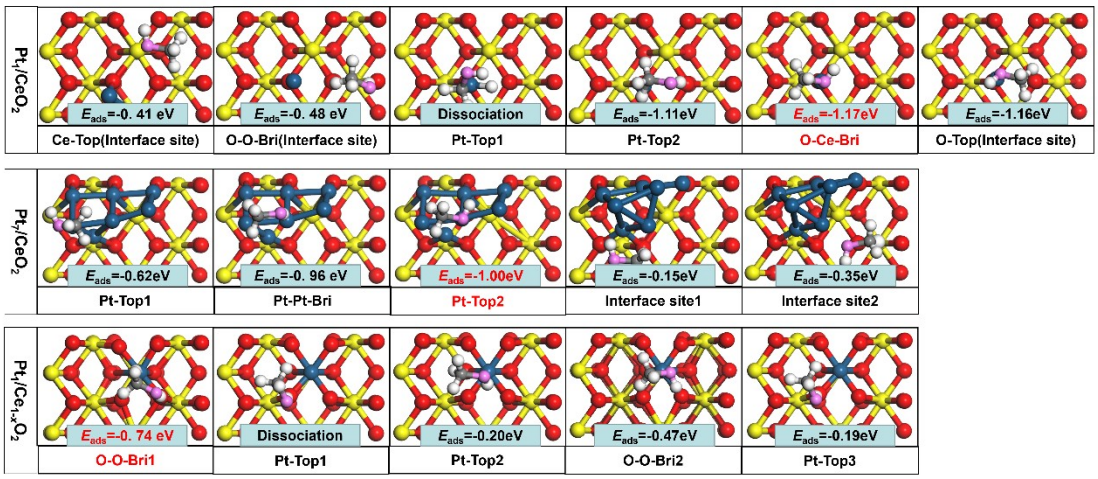

Figure S5. Screening of methanol molecular adsorption sites on Pt_1/CeO_2(110), Pt_7/CeO_2(110), and $Pt_1/Ce_{1-x}O_2$(110). H: white; C: black; O of the CH_3OH molecule:

pink; O of the CeO_2: red; Ce: yellow; Pt: blue.

8. Methanol adsorption.

Table S3. The change of bond lengths before and after methanol adsorption, as well as the adsorption energy and adsorption mode on the surface of different catalysts.

	Adsorption energy (eV)	binding configuration	C-H bond Length (Å)	O-H bond Length (Å)	C-O bond Length (Å)
Gas phase	--	--	1.103	0.971	1.432
Pt_1/CeO_2	1.17	top-bound through oxygen	1.098	0.976	1.457
Pt_7/CeO_2	1.00	top-bound through oxygen	1.100	0.982	1.439
$Pt_1/Ce_{1-x}O_2$	0.74	top-bound through hydrogen	1.134	1.053	1.368

7. Microkinetic modeling analysis of MD reaction

On the basis of DFT calculated results, a microkinetic modeling of MD reaction over $Pt_1/CeO_2(110)$, $Pt_7/CeO_2(110)$ and $Pt_1/Ce_{1-x}O_2(110)$ surfaces are carried out. Based on the reactions (1)-(11) rate equations as below, the equilibrium coverages (θ) of all species are solved by Fortran program, as listed in the Table S7-S9.

(1) $$\frac{d\theta_{CH3OH*}}{dt} = k_1 p_{CH3OH}/p^{\Theta}\theta^* - k_{-1}\theta_{CO*} - k_2\theta_{CH3OH*} + k_{-2}\theta_{CH3O*}\theta_{H*} - k_6\theta_{CH3OH*} + k_{-6}\theta_{CH2OH*}\theta_{H*} = r_1 - r_2 - r_6$$

(2) $$\frac{d\theta_{CH3O*}}{dt} = k_2\theta_{CH3OH*} - k_{-2}\theta_{CH3O*}\theta_{H*} - k_3\theta_{CH3O*} + k_{-3}\theta_{CH2O*}\theta_{H*} = r_2 - r_3$$

(3) $$\frac{d\theta_{CH2O*}}{dt} = k_3\theta_{CH3O*} - k_{-3}\theta_{CH2O*}\theta_{H*} - k_4\theta_{CH2O*} + k_{-4}\theta_{CHO}\theta_{H*} + k_7\theta_{CH2OH*} - k_{-7}\theta_{CH2O*}\theta_{H*} = r_3 - r_4 + r_7$$

(4) $\frac{d\theta_{CHO*}}{dt}=k_4\theta_{CH2O*}-k_{-4}\theta_{CHO}\theta_{H*}-k_5\theta_{CHO*}+k_{10}\theta_{CHOH*}-k_{-10}\theta_{CHO*}\theta_{H*}=r_4-r_5+r_{10}$

(5) $\frac{d\theta_{CO*}}{dt}=k_5\theta_{CHO*}+k_{11}\theta_{COH*}=r_5+r_{11}$

(6) $\frac{d\theta_{CH2OH*}}{dt}=k_6\theta_{CH3OH*}-k_{-6}\theta_{CH2OH*}\theta_{H*}-k_7\theta_{CH2OH*}+k_{-7}\theta_{CH2O*}\theta_{H*}-k_8\theta_{CH2OH*}+k_{-8}\theta_{CHOH*}\theta_{H*}$
$=r_6-r_7-r_8$

(7) $\frac{d\theta_{CHOH*}}{dt}=k_8\theta_{CH2OH*}-k_{-8}\theta_{CHOH*}\theta_{H*}-k_9\theta_{CHOH*}+k_{-9}\theta_{COH*}\theta_{H*}-k_{10}\theta_{CHOH*}+k_{-10}\theta_{CHO*}\theta_{H*}$
$=r_8-r_9-r_{10}$

(8) $\frac{d\theta_{COH*}}{dt}=k_9\theta_{CHOH*}-k_{-9}\theta_{COH*}\theta_{H*}-k_{11}\theta_{COH*}=r_9-r_{11}$

(9) $\frac{d\theta_{H2*}}{dt}=k_{12}\theta_{H*}\theta_{H*}=r_{12}$

(10) $\frac{d\theta_{H*}}{dt}=k_2\theta_{CH3OH*}-k_{-2}\theta_{CH3O*}\theta_{H*}+k_3\theta_{CH3O*}-k_{-3}\theta_{CH2O*}\theta_{H*}+k_4\theta_{CH2O*}-k_{-4}\theta_{CHO*}\theta_{H*}+k_5\theta_{CHO*}+k_6\theta_{CH3OH*}-k_{-6}\theta_{CH2OH*}\theta_{H*}+k_7\theta_{CH2OH*}-k_{-7}\theta_{CH2O*}\theta_{H*}+k_8\theta_{CH2OH*}-k_{-8}\theta_{CHOH*}\theta_{H*}+k_9\theta_{CHOH*}-k_{-9}\theta_{COH*}\theta_{H*}+k_{10}\theta_{CHOH*}-k_{-10}\theta_{CHO*}\theta_{H*}+k_{11}\theta_{COH*}-2k_{12}\theta_{H*}\theta_{H*}$
$=r_2+r_3+r_4+r_5+r_6+r_7+r_8+r_9+r_{10}+r_{11}-2r_{12}$

(11) $\frac{d\theta_{*}}{dt}=-k_1p_{CH3OH}/p^{\Theta}\theta^{*}=-r_1+r_{12}$

Table S4. Reaction rate constant (k_+/k_-) of the elementary reaction step on $Pt_1/CeO_2(110)$ surface under different temperatures.

	373K	423K	473K	523K	573K
k_1	2.49×10^{8}	2.34×10^{8}	2.21×10^{8}	2.10×10^{8}	2.01×10^{8}
k_{-1}	3.33×10^{-3}	2.40×10^{-1}	6.94×10^{0}	1.05×10^{2}	9.76×10^{2}
k_2	5.27×10^{10}	1.53×10^{11}	3.57×10^{11}	7.12×10^{11}	1.27×10^{12}
k_{-2}	3.69×10^{-4}	6.13×10^{-2}	3.45×10^{0}	9.01×10^{1}	1.33×10^{3}
k_3	2.36×10^{2}	3.27×10^{2}	2.61×10^{3}	8.13×10^{5}	1.89×10^{5}
k_{-3}	9.12×10^{6}	4.13×10^{7}	1.36×10^{8}	3.56×10^{8}	7.89×10^{8}
k_4	1.87×10^{0}	8.61×10^{1}	1.77×10^{3}	2.04×10^{4}	1.54×10^{5}
k_{-4}	4.95×10^{-22}	8.02×10^{-18}	1.66×10^{-14}	8.00×10^{-12}	1.31×10^{-9}

k_5	2.28×10^{6}	4.08×10^{7}	4.43×10^{7}	8.58×10^{8}	1.32×10^{9}
k_{-5}	2.09×10^{-21}	8.86×10^{-18}	1.24×10^{-13}	1.26×10^{-11}	4.97×10^{-8}
k_6	2.12×10^{5}	3.18×10^{6}	2.68×10^{7}	1.50×10^{8}	6.26×10^{8}
k_{-6}	1.04×10^{11}	2.49×10^{11}	4.87×10^{11}	8.33×10^{11}	1.29×10^{12}
k_7	2.49×10^{3}	7.80×10^{2}	7.64×10^{3}	1.09×10^{6}	2.25×10^{5}
k_{-7}	1.17×10^{2}	2.14×10^{3}	2.11×10^{4}	1.35×10^{5}	6.23×10^{5}
k_8	3.23×10^{13}	4.65×10^{13}	6.21×10^{13}	7.85×10^{13}	9.53×10^{13}
k_{-8}	3.91×10^{12}	7.24×10^{12}	1.17×10^{13}	1.72×10^{13}	2.37×10^{13}
k_9	4.56×10^{-12}	2.74×10^{-9}	4.28×10^{-7}	2.56×10^{-5}	7.52×10^{-4}
k_{-9}	2.10×10^{3}	1.96×10^{4}	1.15×10^{5}	4.77×10^{5}	1.55×10^{6}
k_{10}	3.51×10^{3}	4.22×10^{4}	3.01×10^{5}	1.48×10^{6}	5.58×10^{6}
k_{-10}	9.21×10^{-3}	4.48×10^{-1}	9.61×10^{0}	1.15×10^{2}	6.81×10^{3}
k_{11}	2.86×10^{-3}	1.82×10^{-1}	4.78×10^{0}	6.74×10^{1}	5.98×10^{2}
k_{-11}	6.00×10^{-24}	2.70×10^{-19}	1.26×10^{-15}	1.16×10^{-12}	3.26×10^{-10}

Table S5. Reaction rate constant (k_+/k_-) of the elementary reaction step on $Pt_7/CeO_2(110)$ under different temperatures.

	373K	423K	473K	523K	573K
k_1	2.49×10^{8}	2.34×10^{8}	2.21×10^{8}	2.10×10^{8}	2.01×10^{8}
k_{-1}	3.07×10^{-2}	1.14×10^{0}	1.95×10^{1}	1.93×10^{2}	1.27×10^{3}
k_2	4.61×10^{4}	2.22×10^{5}	7.82×10^{5}	2.19×10^{6}	5.17×10^{6}
k_{-2}	2.63×10^{4}	1.55×10^{5}	1.04×10^{6}	5.59×10^{7}	5.91×10^{7}
k_3	4.14×10^{10}	4.28×10^{10}	7.26×10^{10}	2.19×10^{11}	6.70×10^{11}
k_{-3}	2.93×10^{8}	1.27×10^{9}	4.02×10^{9}	1.02×10^{10}	2.21×10^{10}
k_4	6.30×10^{11}	1.11×10^{12}	1.76×10^{12}	2.57×10^{12}	3.52×10^{12}
k_{-4}	3.03×10^{3}	4.80×10^{4}	1.58×10^{5}	1.01×10^{6}	3.05×10^{6}
k_5	6.94×10^{9}	2.05×10^{10}	4.83×10^{10}	9.69×10^{10}	1.72×10^{11}
k_{-5}	1.02×10^{7}	5.23×10^{7}	1.89×10^{8}	5.36×10^{8}	1.26×10^{9}
k_6	5.59×10^{2}	4.99×10^{3}	2.85×10^{4}	1.17×10^{5}	3.81×10^{5}
k_{-6}	7.15×10^{3}	7.65×10^{4}	4.94×10^{5}	2.22×10^{6}	7.67×10^{6}
k_7	8.46×10^{8}	2.59×10^{9}	6.30×10^{9}	1.30×10^{10}	2.38×10^{10}
k_{-7}	3.50×10^{-2}	2.80×10^{0}	8.88×10^{1}	1.45×10^{3}	1.46×10^{4}
k_8	5.64×10^{-2}	4.14×10^{0}	1.23×10^{2}	1.93×10^{3}	1.88×10^{4}
k_{-8}	7.02×10^{2}	8.78×10^{3}	8.22×10^{4}	4.02×10^{5}	9.92×10^{5}
k_9	2.48×10^{0}	1.28×10^{2}	2.86×10^{3}	3.56×10^{4}	2.86×10^{5}
k_{-9}	9.01×10^{-17}	3.56×10^{-13}	2.44×10^{-10}	4.80×10^{-17}	3.75×10^{-6}
k_{10}	3.73×10^{2}	2.65×10^{3}	9.82×10^{3}	8.64×10^{4}	3.50×10^{5}
k_{-10}	2.26×10^{-14}	3.49×10^{-11}	1.14×10^{-8}	1.24×10^{-6}	5.97×10^{-5}
k_{11}	1.28×10^{2}	3.34×10^{2}	6.51×10^{3}	5.78×10^{4}	2.97×10^{5}
k_{-11}	2.19×10^{-9}	7.19×10^{-7}	6.95×10^{-5}	2.81×10^{-3}	5.97×10^{-2}

Table S6. Reaction rate constant (k_+/k_-) of the elementary reaction step on Pt_1/Ce_{1-}

$_xO_2$(110) under different temperatures.

	373K	423K	473K	523K	573K
k_1	2.49×10^{8}	2.34×10^{8}	2.21×10^{8}	2.10×10^{8}	2.01×10^{8}
k_{-1}	2.68×10^{4}	4.22×10^{5}	3.66×10^{6}	2.07×10^{7}	8.52×10^{7}
k_2	1.32×10^{15}	9.33×10^{14}	7.14×10^{14}	5.79×10^{14}	4.89×10^{14}
k_{-2}	3.54×10^{1}	1.11×10^{3}	1.70×10^{4}	1.55×10^{5}	9.72×10^{5}
k_3	7.62×10^{8}	1.74×10^{9}	3.37×10^{9}	5.84×10^{9}	9.27×10^{9}
k_{-3}	1.26×10^{-5}	8.91×10^{-4}	2.59×10^{-2}	4.00×10^{-1}	3.87×10^{0}
k_4	2.00×10^{14}	1.30×10^{14}	9.37×10^{13}	7.25×10^{13}	5.92×10^{13}
k_{-4}	1.23×10^{-14}	1.66×10^{-11}	4.89×10^{-9}	4.90×10^{-7}	2.21×10^{-5}
k_5	1.19×10^{7}	6.24×10^{7}	2.32×10^{8}	6.72×10^{8}	1.63×10^{9}
k_{-5}	1.43×10^{-7}	3.77×10^{-5}	3.08×10^{-3}	1.09×10^{-1}	2.09×10^{0}
k_6	5.93×10^{7}	2.60×10^{8}	8.43×10^{8}	2.20×10^{9}	4.86×10^{9}
k_{-6}	7.57×10^{-17}	3.22×10^{-13}	2.35×10^{-10}	4.89×10^{-8}	4.03×10^{-6}
k_7	2.06×10^{12}	2.39×10^{12}	2.70×10^{12}	3.01×10^{12}	3.32×10^{12}
k_{-7}	5.71×10^{5}	2.97×10^{6}	1.10×10^{7}	3.19×10^{7}	7.77×10^{7}

Table S7. Equilibrium coverages (θ) of all species on Pt_1/CeO_2(110) surface under different temperatures.

	373K	423K	473K	523K	573K
θ_{CH3OH*}	0.45×10^{-2}	0.15×10^{-2}	0.61×10^{-3}	0.29×10^{-3}	0.16×10^{-3}
θ_{CH3O*}	0.50×10^{0}	0.52×10^{0}	0.61×10^{0}	0.79×10^{0}	0.89×10^{0}
θ_{CH2O*}	0.12×10^{-6}	0.19×10^{-6}	0.21×10^{-5}	0.11×10^{-2}	0.33×10^{-3}
θ_{CHO*}	0.47×10^{-11}	0.23×10^{-9}	0.57×10^{-8}	0.45×10^{-7}	0.19×10^{-6}
θ_{CO*}	0.89×10^{-14}	0.91×10^{-11}	0.33×10^{-9}	0.80×10^{-7}	0.78×10^{-6}
θ_{CH2OH*}	0.50×10^{-7}	0.22×10^{-6}	0.57×10^{-6}	0.82×10^{-6}	0.10×10^{-5}
θ_{CHOH*}	0.83×10^{-6}	0.29×10^{-5}	0.80×10^{-5}	0.18×10^{-4}	0.38×10^{-4}
θ_{COH*}	0.61×10^{-26}	0.15×10^{-22}	0.86×10^{-20}	0.11×10^{-17}	0.12×10^{-15}
θ_{H*}	0.49×10^{0}	0.48×10^{0}	0.38×10^{0}	0.21×10^{0}	0.11×10^{0}
θ_{*}	0.32×10^{-2}	0.39×10^{-2}	0.21×10^{-2}	0.18×10^{-2}	0.40×10^{-3}

Table S8. Equilibrium coverages (θ) of all species on Pt_7/CeO_2(110) surface under different temperatures.

	373K	423K	473K	523K	573K
θ_{CH3OH*}	0.99×10^{0}	0.98×10^{0}	0.96×10^{0}	0.94×10^{0}	0.89×10^{0}
θ_{CH3O*}	0.11×10^{-5}	0.51×10^{-5}	0.10×10^{-4}	0.94×10^{-5}	0.68×10^{-5}
θ_{CH2O*}	0.74×10^{-7}	0.20×10^{-6}	0.44×10^{-6}	0.84×10^{-6}	0.14×10^{-5}

θ_{CHO*}	0.67×10^{-5}	0.11×10^{-4}	0.16×10^{-4}	0.22×10^{-4}	0.29×10^{-4}
θ_{CO*}	0.12×10^{-2}	0.57×10^{-2}	0.19×10^{-1}	0.48×10^{-1}	0.95×10^{-1}
θ_{CH2OH*}	0.66×10^{-6}	0.19×10^{-5}	0.44×10^{-5}	0.84×10^{-5}	0.14×10^{-4}
θ_{CHOH*}	0.91×10^{-15}	0.20×10^{-12}	0.13×10^{-10}	0.36×10^{-9}	0.51×10^{-8}
θ_{COH*}	0.28×10^{-22}	0.32×10^{-18}	0.50×10^{-15}	0.14×10^{-12}	0.14×10^{-10}
θ_{H*}	0.44×10^{-2}	0.12×10^{-1}	0.16×10^{-1}	0.17×10^{-1}	0.19×10^{-1}
θ_{*}	0.15×10^{-5}	0.13×10^{-6}	0.74×10^{-5}	0.43×10^{-5}	0.63×10^{-5}

Table S9. Equilibrium coverages (θ) of all species on $Pt_1/Ce_{1-x}O_2(110)$ surface under different temperatures.

	373K	423K	473K	523K	573K
θ_{CH3OH*}	0.19×10^{-6}	0.25×10^{-6}	0.31×10^{-6}	0.36×10^{-6}	0.41×10^{-6}
θ_{CH3O*}	0.22×10^{0}	0.12×10^{0}	0.65×10^{-1}	0.36×10^{-1}	0.22×10^{-1}
θ_{CH2O*}	0.83×10^{-6}	0.16×10^{-5}	0.23×10^{-5}	0.29×10^{-5}	0.34×10^{-5}
θ_{CHO*}	0.14×10^{0}	0.18×10^{0}	0.19×10^{0}	0.16×10^{0}	0.10×10^{0}
θ_{CO*}	0.87×10^{-3}	0.58×10^{-2}	0.23×10^{-1}	0.61×10^{-1}	0.11×10^{0}
θ_{CH2OH*}	0.56×10^{-11}	0.29×10^{-10}	0.10×10^{-9}	0.29×10^{-9}	0.66×10^{-9}
θ_{H*}	0.64×10^{0}	0.69×10^{0}	0.72×10^{0}	0.75×10^{0}	0.77×10^{0}
θ_{*}	0.30×10^{-3}	0.56×10^{-3}	0.73×10^{-3}	0.79×10^{-3}	0.26×10^{-3}

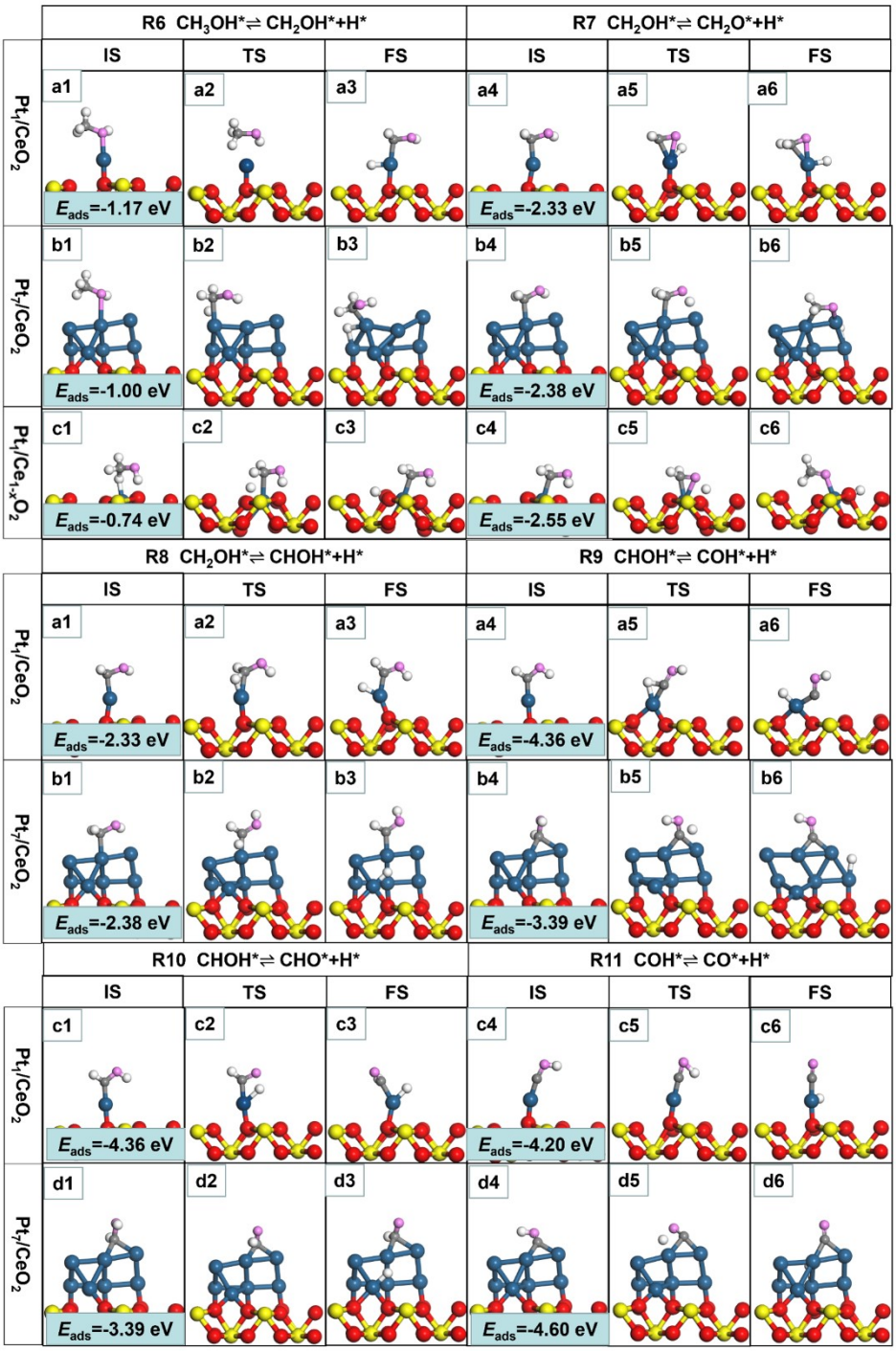

Figure S5. Side view of the initial states (IS), the corresponding transition states (TS) and final states (FS) of R6-R11 on the $Pt_1/CeO_2(110)$, $Pt_7/CeO_2(110)$ and $Pt_1/Ce_{1-x}O_2(110)$ surfaces, along with the adsorption energies (E_{ads}). H: white; C: black; O of the CH_3OH molecule: pink; O of the CeO_2: red; Ce: yellow; Pt: blue.

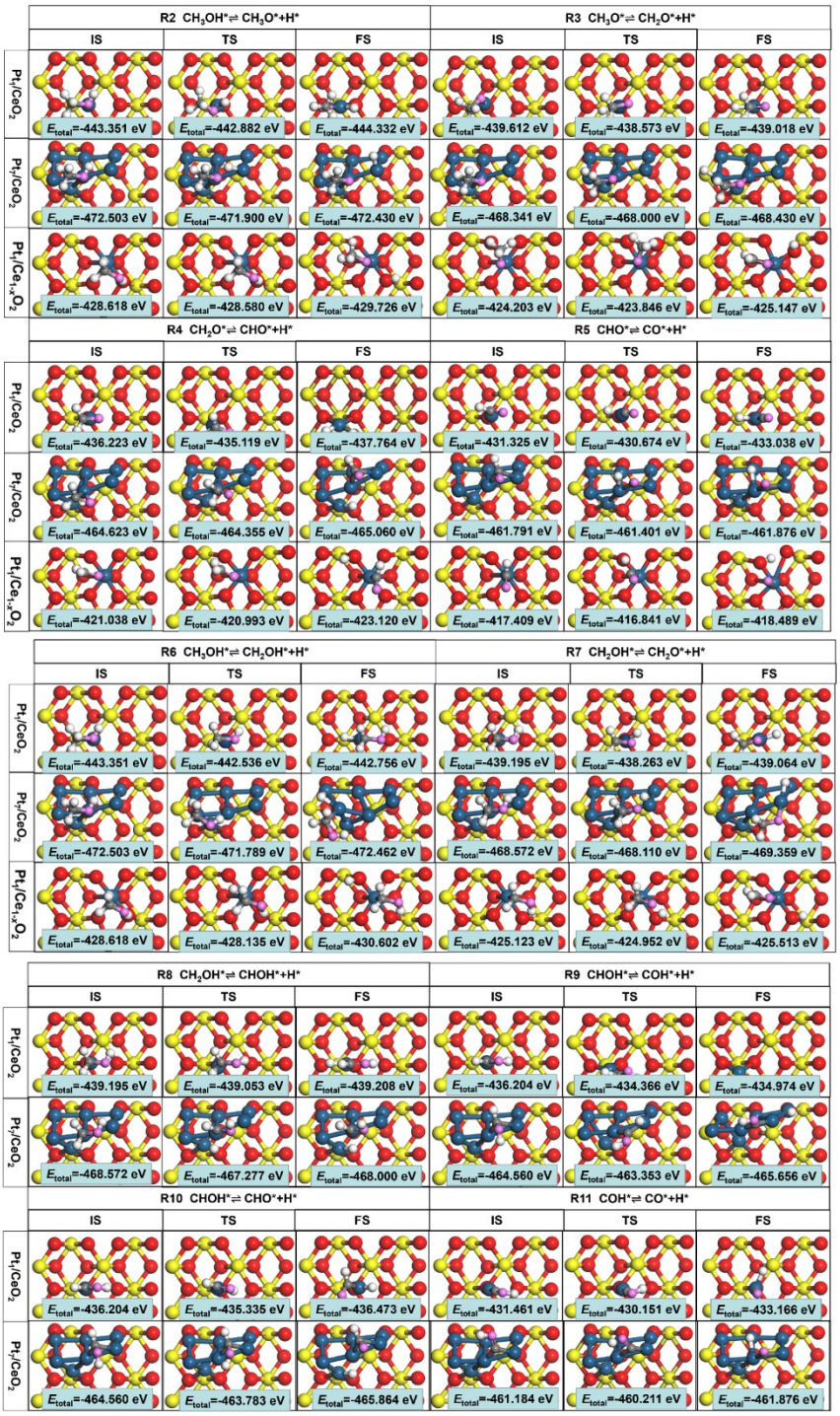

Figure S6. Top view of the initial states (IS), the corresponding transition states (TS) and final states (FS) of R2-R11 on the $Pt_1/CeO_2(110)$, $Pt_7/CeO_2(110)$. H: white; C: black; O of the CH_3OH molecule: pink; O of the CeO_2: red; Ce: yellow; Pt: blue.

Table S10. Comparison of previous work on the mechanism of MD reaction over CeO_2-supported catalysts.

Catalyst	Structural model	Research method	Mechanism	RDS en
$Pt_1/Ce_{1-x}O_2(110)$, $Pt_7/CeO_2(110)$, $Pt_1/Ce_{1-x}O_2(110)$	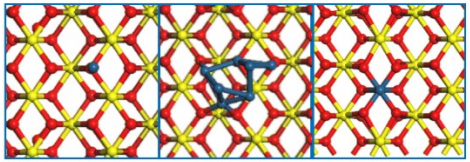	DFT calculations	$CH_3OH \rightarrow CH_3O \rightarrow CH_2O \rightarrow CHO \rightarrow CO$	1. 0. 0.
Pt_1/CeO_2	Pt-CeO_2 interaction is still unclear	DRIFTS	$CH_3OH \rightarrow CH_3O \rightarrow CO$	
$CeO_2(111)$	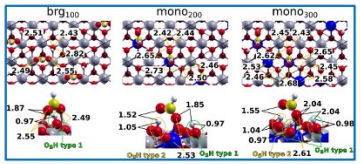	TPSR-IR and DFT	$CH_3OH \rightarrow$ formate	
Cu/CeO_2	Cu clusters loaded on CeO_2	TPD-DRIFTS	$CH_3OH \rightarrow CH_3O \rightarrow$ formate $\rightarrow CO$	
$Ni_3/CeO_2(11\bar{1})$ $Ni_3/CeO_2(\bar{1}1\bar{1})$	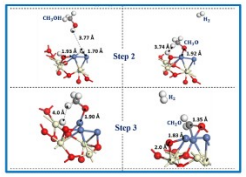	DFT calculations	$CH_3OH \rightarrow CH_3O \rightarrow CH_2O \rightarrow CO$	3. 1.